Ultrasound assisted polymerization for synthesis of ZnO/Polypyrrole composites for zinc/nickel rechargeable battery

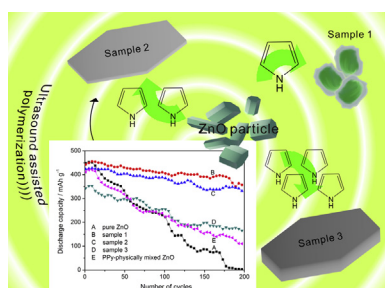Jianhang Huang [a, b], Zhanhong Yang [a, *], Bin Yang [a], Ruijuan Wang [a], Tingting Wang [a]

[a] College of Chemistry and Chemical Engineering, Central South University, Changsha 410083, China
[b] Innovation Base of Energy and Chemical Materials for Graduate Students Training, Central South University, Changsha 410083, China

HIGHLIGHTS

- ZnO/Polypyrrole (PPy) composites with different morphology are synthesized.
- ZnO/PPy composites are utilized as anode material in Zn/Ni rechargeable battery.
- ZnO/PPy composites possess higher capacity retention than that of pure ZnO.

GRAPHICAL ABSTRACT

ARTICLE INFO

ABSTRACT

ZnO/Polypyrrole (PPy) composites are synthesized by ultrasound assisted chemical polymerization of PPy in the presence of ZnO particles. With different initial content of pyrrole, granular and layered ZnO/PPy composite are formed. The fourier transform infrared spectra (FT-IR), X-ray diffraction (XRD), scanning electron microscopy (SEM) and transmission electron microscopy (TEM) are adopted to characterize the as-prepared samples. ZnO/PPy composites are used as anode material for Zn/Ni batteries. Galvanostatic charge/discharge experiments, cyclic voltammograms (CV) and electrochemical impedance spectroscopy (EIS) are conducted to evaluate the cycle performance of electrodes. ZnO/PPy composites show superior capacity stability, more stable charge plateau and higher discharge plateau compared to conventional ZnO electrode. Furthermore, rate performance is also improved by ZnO/PPy composites.

1. Introduction

With the development of electrification era, more and more electric productions are emerging, which require of a reliable, stable and cost effective energy storage device. The zinc/nickel electrochemical system is a promising candidate for alkaline storage batteries owing to its good performance such as high energy density, high power density, high open-circuit-voltage, and a small self-discharge rate [1–3]. What matters more is that the electrode active materials used in the Zn/Ni system are low-toxic and inexpensive materials, and exist in abundance in nature. So the Zn/Ni system is a suitable substitute for the lead-acid and nickel—hydrogen system, and remains a serious candidate for electromobiles. However, the biggest challenge with zinc electrodes is their shape changes and dendrite growth during cycling caused by high solubility of discharge product in alkaline solution, which results in relatively low cycle life of this system [4,5]. In past decades, numerous works have been undertaken to improve the anodic properties of zinc electrode in alkaline solution.

* Corresponding author. Tel.: +86 731 88879616.
E-mail addresses: zhongnan320@gmail.com, zhyang@mail.csu.edu.cn (Z. Yang).

Improvements initiatives in zinc electrode include the use of additives, morphology control of zinc particle and seeking novel active material. Electrode additives include conductive ceramic [6,7], Bi_2O_3 [8], Ag [9], TiO_2 [10], $In(OH)_3$ [11] and so on. The additives, added through the physical entrapment or by localized precipitation of zinc-containing species, can restrain the migration of zincate away from zinc electrode and improve electronic conductivity and current distribution of the zinc electrode [12]. Different morphology of zinc particle, such as nanoplate [13], nanowire [14], nanorod [15], hollow fusiform and hexagonal taperlike ZnO [16], are prepared to investigate their influences on electrochemical character. And some zinc-containing material as active anode material for Zn/Ni rechargeable battery, such as calcium zincate [17] and zinc-containing hydrotalcite [18], were investigated.

Functional organic-inorganic composite with desired properties is an important research field. They provide a new functional hybrid, with synergetic or complementary behavior between organic and inorganic materials, which have attracted considerable attention for their potential applications. As we know, Polypyrrole (PPy), a conducting conjugated polymer, has tremendous potential application due to its low cost, facile synthesis, air and thermal stability, significant electrical conductivity, electrochemical properties and environmentally benign performance. It can be used in following fields: polymeric rechargeable batteries for energy-storage purposes, electrode materials for electrochemical supercapacitors, metal corrosion protection coating materials, matrix for structural composite materials, sensors, gas/humidity testing, electrochromic devices and photovoltaic (solar cell) materials [19,20]. In previous work, Suga et al. [21] proposed that anodes, comprising zinc active material and a polymer layer, could suppress dendrite growth and shape change. Furthermore, dip coating, brush coating and electrodeposition coating of polyaniline or polypyrrole on zinc electrode have been found to be useful in stabilizing the capacity of electrode on repeated cycling [22,23]. In addition, Zhou et al. [24] and Abe et al. [25] investigated the effect of ionomer on zinc electrode. The polymer or ionomer layer on the surface of zinc foil limited the diffusion of the discharge products due to its fine porous structure and re-complexation with zincate ions. In this paper, we prepared ZnO/Polypyrrole (ZnO/PPy) composite using an ultrasound assisted chemical polymerization with the aim to improve cycle life of zinc electrode. The electrochemical behavior of as-prepared ZnO/PPy composite was investigated.

2. Experimental

2.1. Materials preparation

ZnO/PPy composites were synthesized by using a polymerization of the monomer in the present of ZnO particles accompanied by continuous ultrasound and mechanical stir. Compared with conventional magnetic stirring in the polymerization process, ultrasound can provide intense turbulence associated with shear and liquid circulation, it not only results in improved particle distribution of ZnO particles, but also provides a faster dissociation of pyrrole, which generates an enhanced quantum of radicals during the polymerization process and thus gives an improved polymerization efficiency. The pyrrole monomer obtained from Sinopharm Chemical Reagent Co., Ltd. was distilled under reduced pressure. ZnO particles were obtained from Xilong chemical Co., Ltd. Ammonium persulfate (APS), p-toluenesulfonic acid (p-TSA) were both purchased from Sinopharm Chemical Reagent Co., Ltd. NaOH was obtained from Tianjing Chemicala Reagent Research Institute, and they were used as received without further treatment. In a typical synthesis, 0.6 g ZnO was dispersed in 20 mL distilled water under ultrasound. 1.5 mmol sodium p-toluene sulfonate (prepared from NaOH and p-toluenesulfonic acid) and 1.85 (sample 1), 3.7 (sample 2) and 7.4 (sample 3) mmol pyrrole monomer were added to above ZnO suspended solution under constant sonication and continuously stirred for 5 min. Afterward, 0.9 mmol Ammonium persulfate was promptly mixed into the above solution at room temperature. The resulting solution was kept under ultrasound and stir for 40 min. During the polymerization, the color of the system changed from white to grey slowly, and the more the initial pyrrole content, the blacker the color of sample: sample 3 is blacker than sample 2 which is blacker than sample 1. The products were filtered and washed thoroughly with distilled water (to remove the unreacted ammonium persulfate and sodium p-toluene sulfonate) and then with methanol (to remove the oligomers). The filtered sample was dried in a vacuum oven at 333 K for further analysis. The amount of polymer in the total composition is determined by the mass difference before and after calcinations treatment of samples in the oxygen atmosphere at 873 K for 90 min. The content of polymer for sample 1, sample 2 and sample 3 is 5.1%, 11.4% and 16.8% respectively. Pure PPy was also synthesized following the same procedure as described before but without ZnO, and PPy-physically mixed ZnO with 11.4% PPy was synthesized in order to compare its electrochemical property with ZnO/PPy composites.

2.2. Characterization of ZnO/PPy composites

Fourier transform infrared (FT-IR) spectroscopy of as-prepared samples was conducted on a Nicolet Nexus-670 FT-IR spectrometer (as KBr discs, with wave number 400–4000 cm^{-1}). The morphology and structure were observed on scanning electron microscope (SEM) (JSM-6360LV) and transmission electron microscope (TEM) (JEOL-2010). The X-ray diffraction (XRD) pattern was conducted using X-ray diffractometer (Philips X' Pert Pro).

2.3. Preparation of ZnO/PPy electrodes

For fabrication of ZnO/PPy electrodes, 85 wt. % of ZnO/PPy powder was mixed with 10 wt. % acetylene black and 5 wt. % Polytetrafluoroethylene (PTFE) (served as conductive agent and binder respectively). And the mixture was grinded with agate mortar until it became muddy mixture with proper viscosity. Then above muddy mixture was incorporated to a copper mesh which served as current collector. For comparison, similar zinc electrode with pure ZnO was fabricated. The obtained electrodes were dried at 333 K in a vacuum oven for further testing. And the weight of active material in negative zinc electrode is about 30 mg per electrode.

2.4. Electrodes testing

For galvanostatic charge/discharge cycle test, a two-electrode cell was adopted, which includes working electrode and counter electrode, but without reference electrode compared with a three-electrode system. The capacity of chosen counter electrode (sintered $Ni(OH)_2$ electrode) was three times higher than working electrode in the aim of making sure that the capacities of cells was controlled by working electrode. In addition, 6.0 M KOH solution with saturated ZnO was used as the electrolyte, multilayer polypropylene micro-porous membranes as the separator. The two-electrode system were charged at 1 C (or 3 C) for 60 min (or 20 min) and discharged at 1 C (or 3 C) down to 1.2 V cut-off, the current for 1 C is about 14 mA. Cycle test was performed with a battery test apparatus NEWWARE BTS-610 (Newware Technology Co., Ltd., China).

For cyclic voltammetry test (CV) and electrochemical impedance spectroscope (EIS), a three-electrode cell was used with an Hg/HgO

electrode as the reference electrode, a sintered $Ni(OH)_2$ electrode as counter electrode, and as-prepared ZnO/PPy electrodes as the working electrode. The CV test was performed over the rage from −1.65 V to −0.85 V, at a scanning rate of 20 mV s^{-1}. EIS was conducted over the frequency range from 100 kHz to 0.01 Hz, the amplitude of the ac potential perturbation was 5 mV. And EIS data was fitted using the software of Zview. Above testing were conducted with RST 5000 (Zhengzhou Shiruisi Technologh Co., Ltd.) electrochemical workstation.

3. Results and discussions

3.1. Characterization of the ZnO/PPy composites

The FT-IR spectra of pure PPy, sample 1, sample 2 and sample 3 are shown in Fig. 1. For pure PPy(curve A), the specific bands are observed at 1556, 1477, 1313, 1195, 1045 and 916 cm^{-1}. They are close to those reported data [26,27]: stretching vibration (1556 cm^{-1}) of C=C bond, stretching vibration (1313 cm^{-1}) of C−C bond, and bonds (1477, 1195, 1045, 916 cm^{-1}) of pyrrole ring. For the sample 1(curve B), the strongest absorption band at 440 cm^{-1} is assigned to the Zn−O bond due to the high content of ZnO particle. Although the intensity of the absorption bands of sample 1 between 500 and 1600 cm^{-1} is low, some absorption bands can indicate the existence of PPy, such as conjugated double bond at 1646, 1585 and 1220 cm^{-1}, which show a broadening and a shift towards high wave number compared with pure PPy. For the sample 2 and sample 3 (curve C and curve D), the band corresponding to Zn−O bond around 440 cm^{-1} almost disappears while two new strong absorption bands at 1156 and 1118 cm^{-1} arise. These phenomena suggest that there is a strong chemical interaction between PPy and ZnO to form new composite. And the bands at 1156 and 1118 cm^{-1} are assigned to the coordination bond between zinc and nitrogen. The reason for this kind of strong chemical reaction can possibly be attributed to the ultrasound during the synthesis process. The mechanical effects of ultrasound (intense turbulence associated with shear and liquid circulation) not only provides improved particle distribution, but also provides a faster dissociation of initiator which generates an enhanced quantum of radicals during the polymerization process and thus gives a strong chemical reaction with ZnO [28].

Fig. 2 shows the XRD pattern of pure ZnO, sample 1, sample 2 and sample 3. For pure ZnO (curve A), all the peaks match well
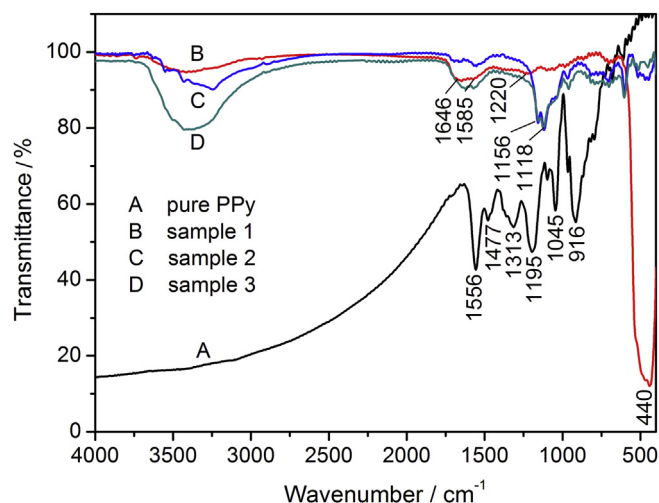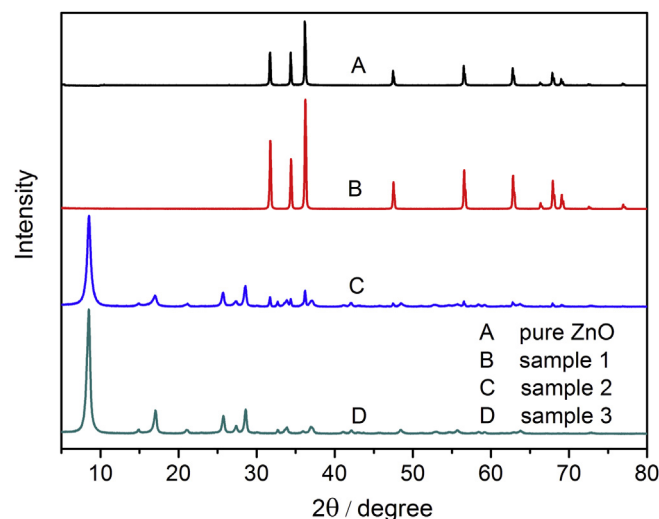
Fig. 2. XRD pattern of pure ZnO (curve A), sample 1 (curve B), sample 2 (curve C) and sample 3 (curve D).

with the standard ZnO with the hexagonal wurtzite structure (JCPDS card 36-1451). With comparison to the XRD pattern of sample 1 (curve B), there is no obvious difference observed. The sharp diffraction peak suggests that sample 1 has good crystalline nature, which implies that a small amount of PPy has no obvious effect on the crystal structure of ZnO. On the other word, PPy may just interact with the surface of ZnO particles, and there is no new critical structure formed. For the sample 2 and sample 3 (curve C and curve D), the XRD patterns are very different with that of sample 1 and pure ZnO. The diffraction peaks of ZnO are subjected a radical shrink, and four diffraction peaks arise at 8.5°, 17°, 26°, 28.5°, respectively. That means there is new structure formed, it is consistent with the result of FT-IR. The only difference between sample 1, sample 2 and sample 3 is the initial pyrrole content added in the preparation process, so we can say that the more content of pyrrole can react with ZnO particle during the polymerization process and form new composite with new crystal structure.

Fig. 3 show the morphology images of pure ZnO(a), sample 1(b), sample 2(c) and sample 3(d). As shown in Fig. 3a, the conventional ZnO particle is a hexagonal prism with the average length about 300 nm. And the appearance of sample 1 shown in Fig. 3b is similar to that of pure ZnO particle, which prove that a small quality of pyrrole has no significant impact on morphology of ZnO. Thus, we provide the TEM images of pure ZnO (inset of Fig. 3a) and sample 1 (inset of Fig. 3b) to further understand the difference between them. As shown in the inset of Fig. 3a, the particle edge of ZnO is clean and smooth. Compared with the inset of Fig. 3b, the particles with dark color are ZnO particles, and the corrugations around the oxide core should be the polypyrrole. The ZnO particle is coated with a layer of PPy film, this result is consistent with the assumption from FT-IR and XRD result.

From Fig. 3c and d, it can be seen that the sample 2 and sample 3 both have hexagonal layer morphology although some plates are incomplete. This morphology is entirely different with pure ZnO and sample 1. From the FT-IR results and XRD pattern, it is sure that ZnO formed a new crystal structure with PPy. And it is noticed that the plate of sample 3 is thicker than sample 2, it results from the more initial pyrrole content. In addition, there are some small particles distributed on the surface of layer, it could be the excessive ZnO particles. The diagrammatic drawing of preparation process of sample 2 and sample 3 is presented in Fig. 4.
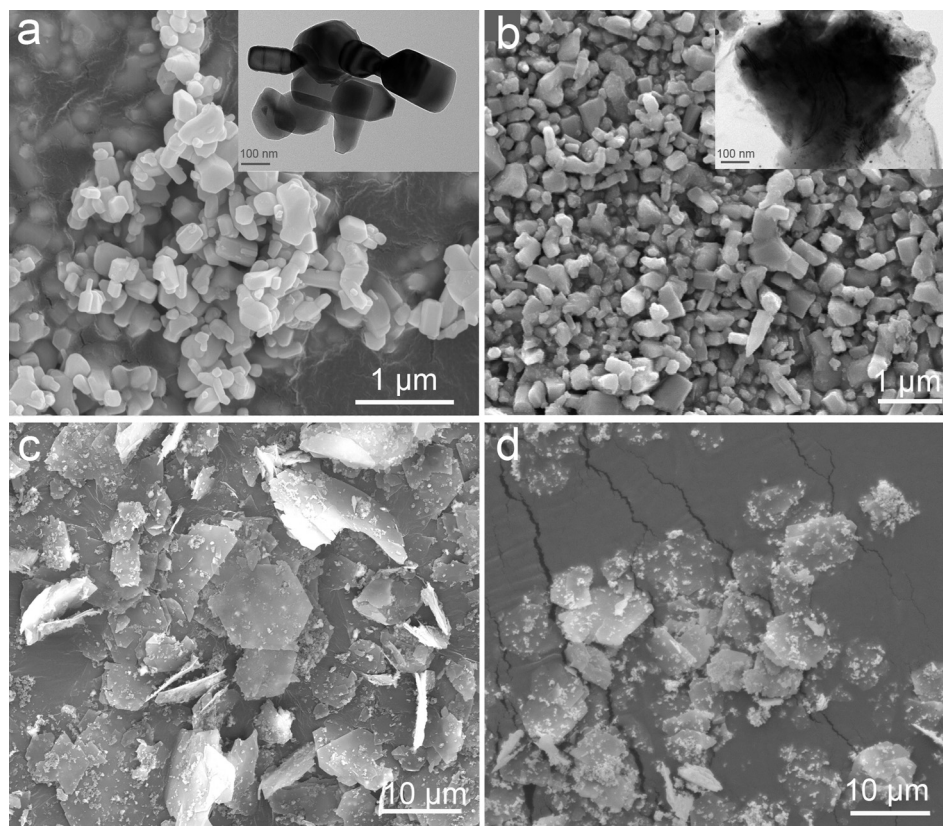
Fig. 1. FT-IR spectra of pure PPy (curve A), sample 1 (curve B), sample 2 (curve C) and sample 3 (curve D).

Fig. 3. SEM images of (a) pure ZnO particles (inset: TEM images of pure ZnO particles); (b) sample 1 (inset: TEM images of sample 1); (c) sample 2; (d) sample 3.

3.2. Cycle performance

Electrochemical cyclic performance of the pure ZnO electrode(curve A), sample 1 electrode(curve B), sample 2 electrode(curve C), sample 3 electrode(curve D) and PPy-physically mixed ZnO (curve E) at current rate of 1 C is shown in Fig. 5a. For the pure ZnO electrode, the discharge capacity achieves the maximum 456 mAh g^{-1} at the 7th cycle. Despite it possesses high discharge capacity at first several cycles, it suffers from rapid capacity fade. As we can see from curve A, after 178 cycles, the pure ZnO electrode almost completely loses its efficacy. In comparison with the pure ZnO, although the highest capacity of ZnO/PPy electrodes is lower,
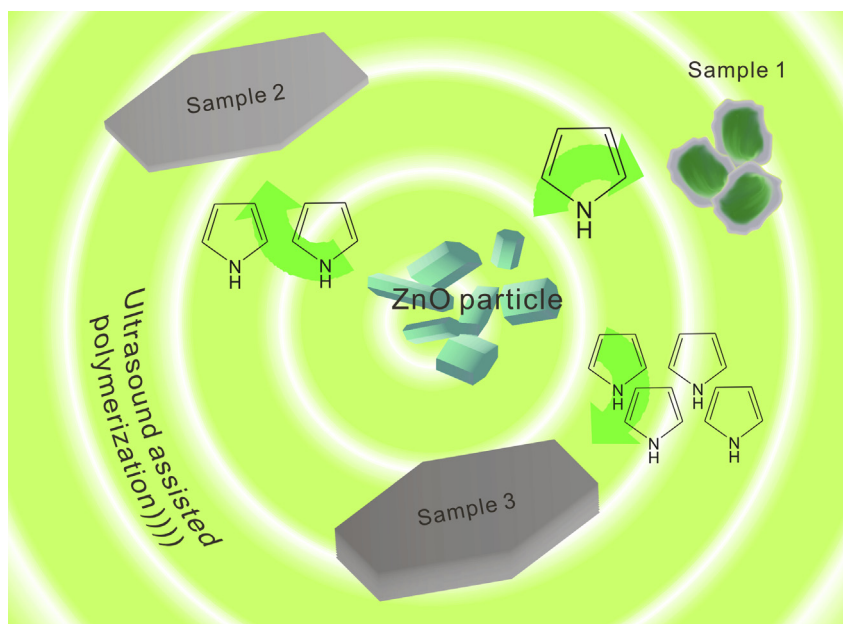

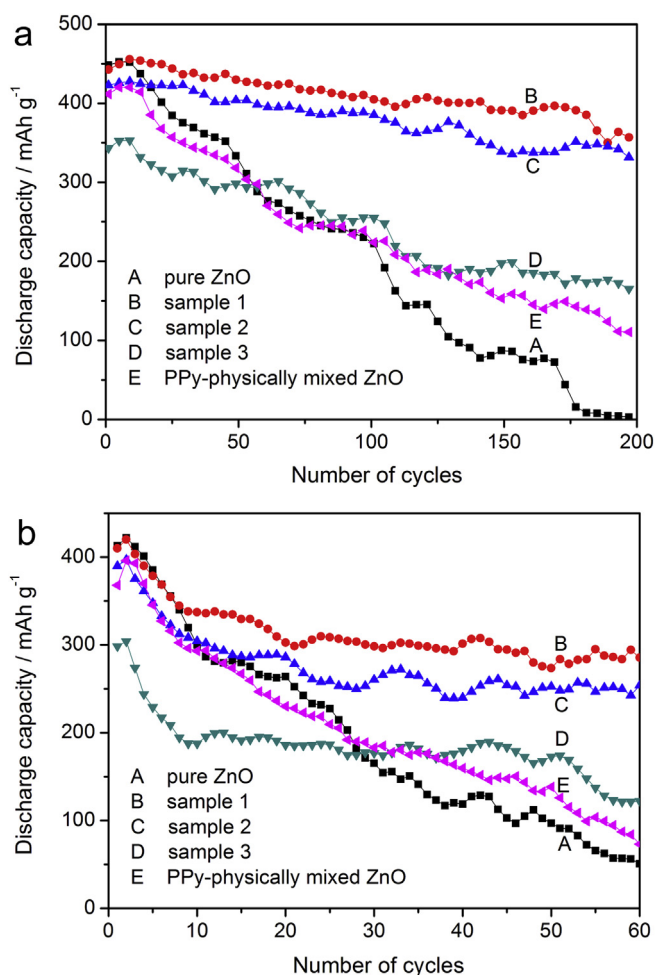**Fig. 4.** The diagrammatic drawing of preparation process.

Fig. 5. Cycle performance of pure ZnO (curve A), sample 1 (curve B), sample 2 (curve C), sample 3 (curve D) and PPy-physically mixed ZnO (curve E) at current rate of 1 C (a) and 3 C (b).

the stability is remarkably superior. After 200 cycles, the discharge capacity of sample 1 and 2 electrode decrease to 350 mAh g^{-1} and 332 mAh g^{-1} with a capacity fading rate of 15.3% and 14.5%, respectively. After 15th cycle, both sample 1 and 2 electrodes present higher capacity than that of pure ZnO. Furthermore, the average discharge capacity of sample 1 and 2 electrode is 408 and 380 mAh g^{-1} for the 200 cycling test, and 203 and 175 mAh g^{-1} higher than 205 mAh g^{-1} of pure ZnO electrode, respectively. The essential reason for short lifetime of Zn electrode is dissolution of ZnO in the alkaline electrolyte. Hence, any approach to improving the lifetime should be directed at the retainment of oxidized species at electrode. From above results, the ZnO/PPy composite electrodes are effective in retaining the oxidized species at electrode. The reason is that the PPy film around the ZnO core avoids direct contact with electrolyte, and limits the diffusion of discharge products. Furthermore, for the layered ZnO/PPy composite, zinc–nitrogen coordination interaction of ZnO/PPy composite could make the oxidized products under control in electrode rather than dissolve in electrolyte [22]. It can be noticed that the capacity of sample 2 electrode is about 30 mAh g^{-1} lower than that of sample 1. This phenomenon is associated to the initial amount of pyrrole in preparation process which decreases the percentage of ZnO in the electrode. And for sample 3, the discharge capacity is much lower than sample 1 and sample 2 because of the increasing content of PPy, the average capacity of sample 3 is 243 mAh g^{-1}. So

the superiority of sample 3 with high PPy content is not obvious compared with 205 mAh g^{-1} of pure ZnO electrode. In addition, although PPy-physically mixed ZnO (curve E) exhibits better capacity-retainment than pure ZnO (110 mAh g^{-1} after 200 cycles), it is still far behind the sample 1 and sample 2. This is because that the mechanical mixing cannot provide uniform mixing with ZnO, leading to low utilization of PPy. Compared with mechanical mixing, ultrasound assisted chemical polymerization not only make the PPy distribute uniformly, but also change the surface states and structure of ZnO particles, these changes play an important role in inhibiting dissolution of discharge product and growth of dendrite.

As we know that the rate performance of ZnO anode is poor. And a high rate capability is important in meeting the needs of high-storage applications. So we evaluate the electrochemical performance at high discharge current densities. Fig. 5b shows the electrochemical cyclic performance of the pure ZnO electrode (curve A), sample 1 electrode (curve B), sample 2 electrode (curve C), sample 3 electrode(curve D) and PPy-physically mixed ZnO (curve E) at current rate of 3 C. We can see that the discharge capacity of all testing electrodes decrease rapidly at first several cycles. But the three electrodes of ZnO/PPy composites retain the discharge capacity well after tenth cycle while the pure ZnO and PPy-physically mixed ZnO electrode continues the rapid fading of discharge capacity. The discharge capacity of pure ZnO, PPy-physically mixed ZnO, sample 1, sample 2 and sample 3 electrode decreases to 51 mAh g^{-1}, 73 mAh g^{-1}, 285 mAh g^{-1}, 254 mAh g^{-1} and 122 mAh g^{-1} respectively after 60 cycles. And the according discharge capacity fading rate of pure ZnO and PPy-physically mixed ZnO electrode is 87.9% and 81.6% respectively, they are much higher than that of sample 1, sample 2 and sample 3 electrodes which is 32.1%, 36.0% and 59.0% respectively. These results indicate that ZnO/PPy composites show much more mild capacity fade compared to the significant drop of discharge capacity of pure ZnO. The rapid fading of pure ZnO and PPy-physically mixed ZnO electrode is attributed to the large concentration polarization caused by high current rate, which accelerates the dissolution of oxidized species into electrolyte. For pure ZnO electrode, the non-uniform deposition of oxidized species promotes the growth of zinc dendrite and shape change of electrode during cycle process, which can in turn increase the polarization and decrease the utilization rate of active material. Then forming a vicious circle finally, leading to the dramatic capacity fading of pure ZnO electrode. For PPy-physically mixed ZnO, the un-uniform distribution of PPy make it has no obvious improvement on cycle performance at high rate. But for ZnO/PPy electrode, the dissolution of oxidized species is effectively suppressed, it can break the vicious circle, resulting in higher discharge capacity than pure ZnO electrode.

Fig. 6 shows the morphology of pure ZnO (a), samples 1 (b), 2 (c), 3 (d) and (e) PPy-physically mixed ZnO after 200 cycles. As shown in Fig. 6(a), zinc dendrite can be clearly observed, which implies that local current concentration, non-uniform current distribution, occurred on the electrode surface [25]. This is one important reason why the discharge capacity of pure ZnO electrode decline quickly. In contrast, although there is little zinc dendrite formed in Fig. 6(b), granular morphology of sample 1, 2 and 3 after 200 cycles are observed which is completely different from that of pure ZnO at the same magnification, indicating that ZnO/PPy composites is effective in suppressing growth of zinc dendrite. Generally, granular structure is preferable for zinc electrode, because it possesses advantages such as better current collecting and smaller volumetric change during charge/discharge cycles [25]. So, the as-prepared ZnO/PPy composites exhibit much better capacity retention than that of pure ZnO. In addition, we can see in Fig. 6(e) that PPy-physically mixed ZnO exhibit zinc dendrite like pure ZnO electrode, which indicates PPy-physically mixed ZnO has no obvious
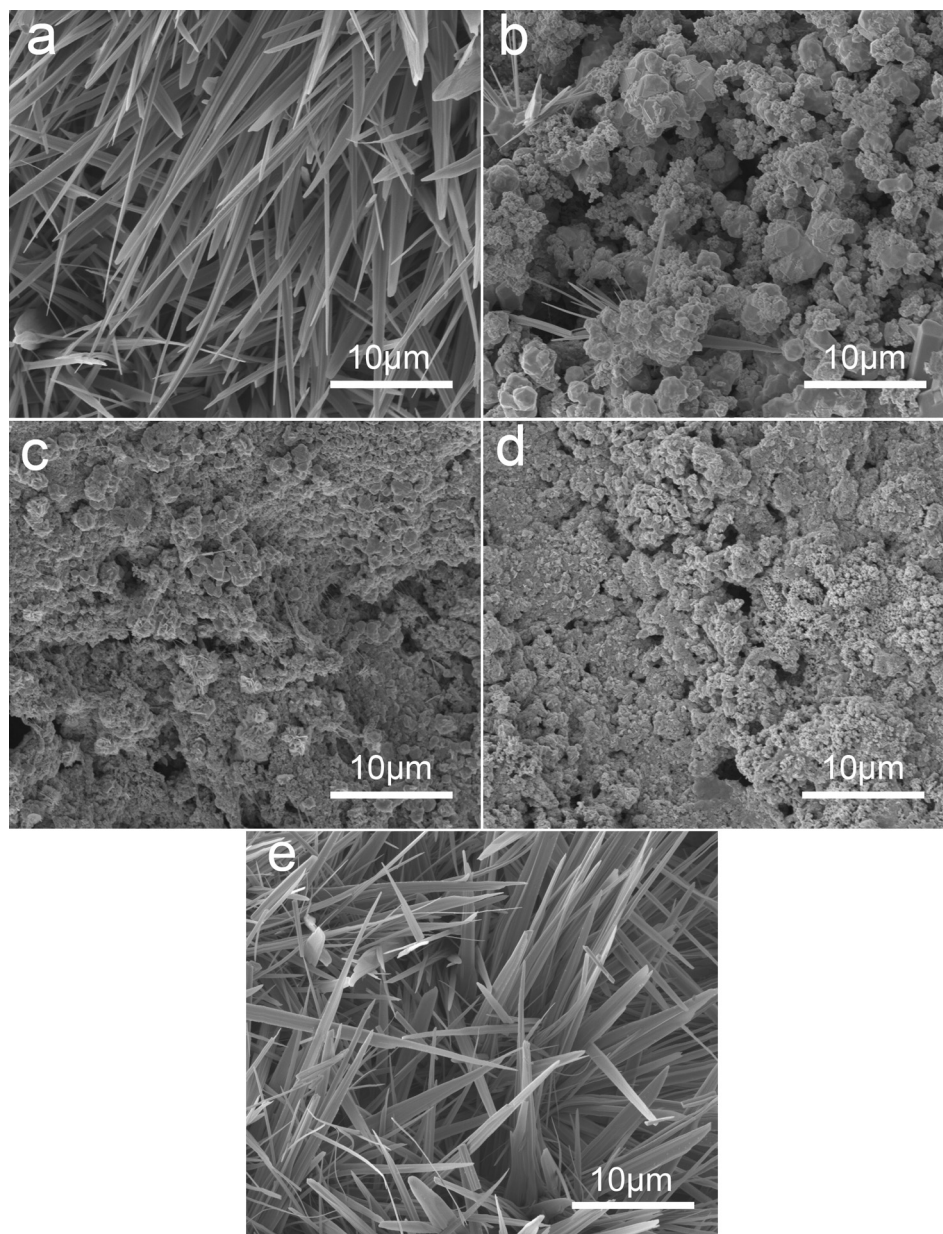
Fig. 6. SEM images of (a) pure ZnO, (b) sample 1, (c) sample 2, (d) sample 3 and (e) PPy-physically mixed ZnO after 200 cycles.

inhibiting effect on dendrite growth due to the disadvantage of physical mixture.

Fig. 7 shows the XRD patterns of pure ZnO (cuve A), samples 1 (cuve B), sample 2 (cuve C), sample 3 (cuve D) and PPy-physically mixed ZnO (curve E) after 200 cycles. For pure ZnO electrode and PPy-physically mixed ZnO after 200 cycles, peaks assigned to Zn can also be observed in addition to the diffraction peaks assigned to ZnO, these diffraction peaks of Zn indicate the existence of zinc dendrite. Besides, there is one broad weak peak around 26° for PPy-physically mixed ZnO, it is assigned to PPy. As to ZnO/PPy composites, the diffraction peaks of Zn are weak, which demonstrate the growth inhibitory effect of composite on zinc dendrite. Furthermore, the intensive peak at 8.5° for ZnO/PPy composites disappear, it could be associated with the destruction of layer morphology after 200 cycles. But there are still two peaks for composite remained at 17° and 26°, meaning that although some part of composite were changed to ZnO during the cycling process,

there is ZnO/PPy composites remained after 200 cycles, which illustrate that the structure of composite is another important factor to affect the cycle performance in addition of the amount of PPy.

3.3. Cyclic voltammograms of ZnO/PPy electrodes

CV analysis is helpful to understand the effects of PPy on the electrochemical performance of ZnO. The comparison of the cyclic voltammograms obtained from pure ZnO electrode and ZnO/PPy composite electrodes after ten cycles are given in Fig. 8. The potential scan is initiated in the positive direction from the potential -1.65 V at a scan rate of 20 mV s^{-1}. For pure ZnO electrode (curve A) and PPy-physically mixed ZnO (curve E), there is an anode peak at -1.190 V and -1.194 V respectively corresponding to the oxidation of Zinc deposited during the discharge process. And a cathodic peak is observed at -1.472 V and -1.466 V respectively
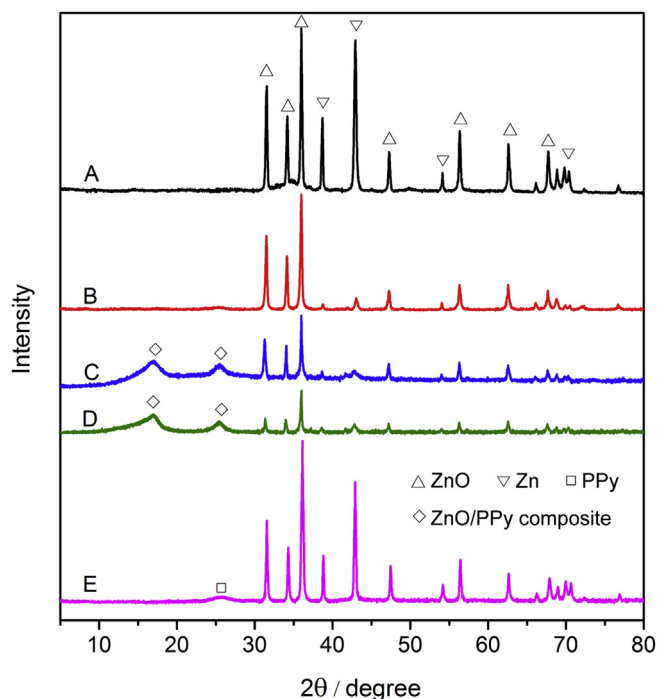
Fig. 7. XRD pattern of pure ZnO (curve A), sample 1 (curve B), sample 2 (curve C), sample 3 (curve D) and PPy-physically mixed ZnO (curve E) after 200 cycles. △: ZnO ▽: Zn □: PPy ◇: ZnO/PPy composite.

corresponding to the reduction of ZnO. For ZnO/PPy composite electrodes (sample 1: curve B, sample 2: curve C, sample 3: curve D), the oxidation of Zn gives rise to anodic peak at −1.214 V, −1.213 V and −1.20 V, respectively. As we can see that anode peak potential of ZnO/PPy composites is more negative compared to pure ZnO and PPy-physically mixed ZnO electrode, it can be caused by the small polarization which results from the suppressed dendrite growth by the surface modification and structure changes of ZnO. But the anode peak potential of sample 3 shifts toward positive direct compared to sample 1 and sample 2, this is due to the increasing content of PPy which may handicap the ion diffusion. When the potential scan is switched to the negative direction at −0.85 V, reduction peak is observed at −1.466, −1.474 V and −1.482 V for sample 1, sample 2 and sample 3. From above we

can calculate the potential interval between anodic and cathodic peak: 0.282 V, 0.272 V, 0.252 V, 0.261 V and 0.282 V for pure ZnO, PPy-physically mixed ZnO, sample 1, sample 2 and sample 3, respectively. As we know that the potential interval is a measurement of reversibility, the lower potential interval means the higher electrochemical kinetics of redox process, leading to higher reversibility. So the electrode of sample 1 and sample 2 possess better reversibility than pure ZnO, PPy-physically mixed ZnO and sample 3.

It can be noticed that there is another additional anodic peak around −1.09 V for ZnO/PPy electrodes, while PPy-physically mixed ZnO exhibits a week broad peak around −1.04 V. But the pure ZnO has no similar anodic peak. This phenomenon could be ascribed to the multi step of anodic dissolution [8,29] which could be described according to following equations:

$$Zn + 4OH^- = Zn(OH)_4^{2-} + 2e \qquad (1)$$

$$Zn + 3OH^- = Zn(OH)_3^- + 2e \qquad (2)$$
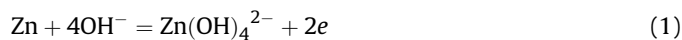
It is obvious that Equation (1) must be the one taking place in the first anodic peak. The concentration of OH^- near the surface of electrode will decrease in the Equation (1) proceeding. On this occasion, the existence of PPy leads to an inadequate contact between active material and OH^- at reaction layer, then the anodic reaction will take place in terms of Equation (2), which is in accordance with the peak around −1.09 V.

3.4. The galvanostatic charge/discharge curves analysis of zinc electrodes

Fig. 9a and b shows the typical charge/discharge curve of pure ZnO electrode (curve A), sample 1 electrode (curve B), sample 2 electrode (curve C), sample 3 electrode (curve D) and PPy-physically mixed ZnO (curve E) at tenth cycle at current rate of 1 C. And the typical charge/discharge curves at current rate of 3 C are shown in Fig. 9c and d. Whether for current rate of 1 C, or for 3 C, it can be noticed that the charge curves of pure ZnO, sample 3 and PPy-physically mixed ZnO arise faster in comparison with that of sample 1 and sample 2. And the discharge plateau voltage of sample 1 and sample 2 are also higher than that of pure ZnO, sample 3 and PPy-physically mixed ZnO. It is well known that the charge/discharge reaction of Zinc electrodes is accompanied with redox reaction, dissolution and electrodeposition. For the charge reaction, reduction and electrodeposition of ZnO occur, and the non-uniform electrodeposition of ZnO cause the growth of zinc dendrite, leading to an increase in the electrochemical polarization, this is why the charge plateau voltage of pure ZnO rise fast. But for ZnO/PPy composite, the special structure of ZnO/PPy composite make the electrodeposition uniform due to re-complexation of zincate ions with imine bonds of the PPy, that will suppress electrochemical polarization and make the charge plateau voltage more stable. On the other hand, the small polarization could also enhance the efficiency of discharge performance, increase the discharge plateau voltage. In addition, irreversible capacity can be obviously observed. The occurrence of irreversible capacity in Fig. 9 is resulted from capacity loss of electrode and the shrinkage of practical capacity compared to theoretical capacity. Because of the polarization of zinc electrode, a part of charging current was expended by polarization, leading to irreversible capacity.

3.5. Electrochemical impedance spectroscopy study

Electrochemical impedance measurements were performed on ZnO/PPy electrodes and pure ZnO electrode after ten cycles. As it
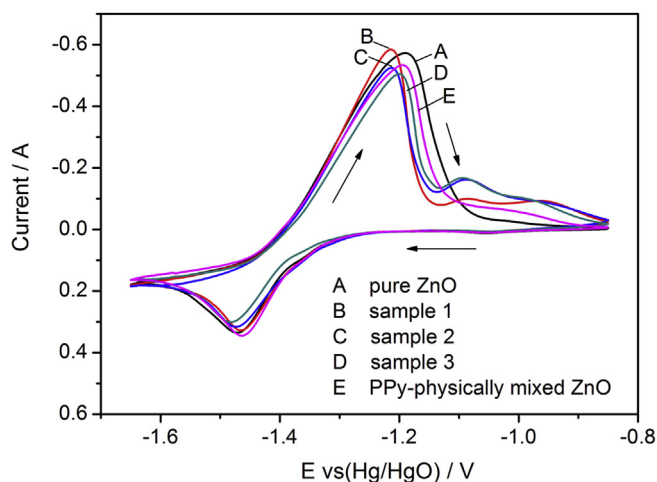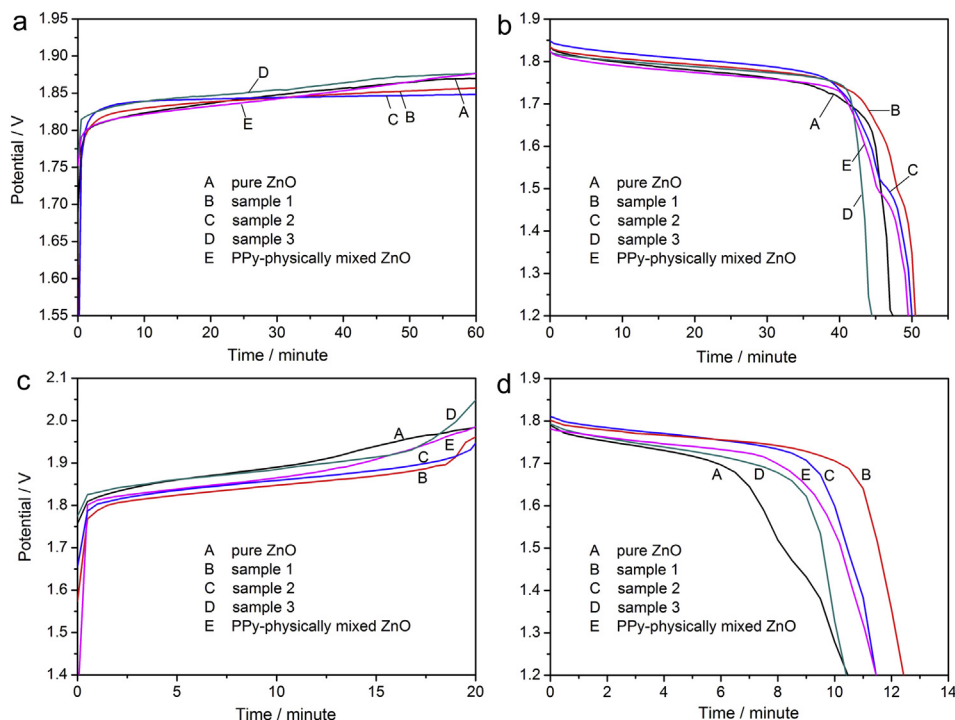

Fig. 8. Cyclic voltammograms of pure ZnO (curve A), sample 1 (curve B), sample 2 (curve C), sample 3 (curve D) and PPy-physically mixed ZnO (curve E).

Fig. 9. (a) Typical charge curves of pure ZnO (curve A), sample 1 (curve B), sample 2 (curve C), sample 3 (curve D) and PPy-physically mixed ZnO (curve E) at current rate of 1 C; (b) Typical discharge curves of pure ZnO (curve A), sample 1 (curve B), sample 2 (curve C), sample 3 (curve D) and PPy-physically mixed ZnO (curve E) at current rate of 1 C; (c) Typical charge curves at current rate of 3 C; (d) Typical discharge curves at current rate of 3 C.

can be seen from the corresponding Nyquist plots (Fig. 10), the impedance response of the five testing electrodes is characterized by the presence of a semi-circle arc in the higher frequency region and a straight line in the lower frequency region. The high-frequency arc has been associated with the double-layer capacitance (CPE) in parallel with the charge-transfer resistance (R_{ct}) at the contact interface between electrode and electrolyte solution. At lower frequencies, there is a straight line having an angle of 45° with the real axis corresponding to Warburg impedance (Z_w) which is characteristics of the semi-infinite diffusion. In order to determine the charge-transfer resistance (R_{ct}), we adopt a

Randles–Ershler type equivalent circuit [30], where R_s is the total ohmic resistance of the solution, CPE is the double layer capacity, R_{ct} is the charge-transfer resistance of the electrode, Z_w is the Warburg impedance. According to the equivalent circuit, the R_{ct} of pure ZnO, PPy-physically mixed ZnO, sample 1, sample 2 and sample 3 electrode are respectively 37.4 Ω, 32.0 Ω, 9.3Ω, 13.9 Ω and 21.4 Ω, and the Warburg resistance are respectively 0.032Ω, 0.037Ω, 0.43Ω, 0.62Ω and 0.96Ω. The charge-transfer resistance of ZnO/PPy electrodes is much lower than that of pure ZnO and PPy-physically mixed ZnO electrode. Specially, PPy-physically mixed ZnO has little decrease of charge-transfer resistance compared to pure ZnO, meaning the utilization of PPy is very low due to non-uniform distribution. The Warburg resistance of ZnO/PPy composites is higher than that of pure ZnO and PPy-physically mixed ZnO, and it increases with increasing content of PPy in composite. The lower charge-transfer resistance of ZnO/PPy composites is due to enhancement in the mobility of electrons owing to highly extended chain conformation of PPy, also attributed to the conjunction and synergistic effect of PPy and ZnO [22,31]. The smaller charge-transfer resistance means a faster kinetics process of electrode, and the electrochemical reaction of ZnO/PPy electrodes is easier to happen compared to pure ZnO and PPy-physically mixed ZnO electrode. But with increasing content of PPy, the Warburg resistance increase, which means the existence of PPy layer slow the ion diffusion. So the results indicate that Sample 1 and Sample 2 are appropriate to be used as anode material for Zn/Ni rechargeable battery.

4. Conclusions

The ZnO/PPy composites are successfully synthesized with the assistance of ultrasound. FT-IR and XRD analysis clearly confirm that sample 1 with low initial content of pyrrole retains the crystal structure of ZnO, but for sample 2 and sample 3 with increasing
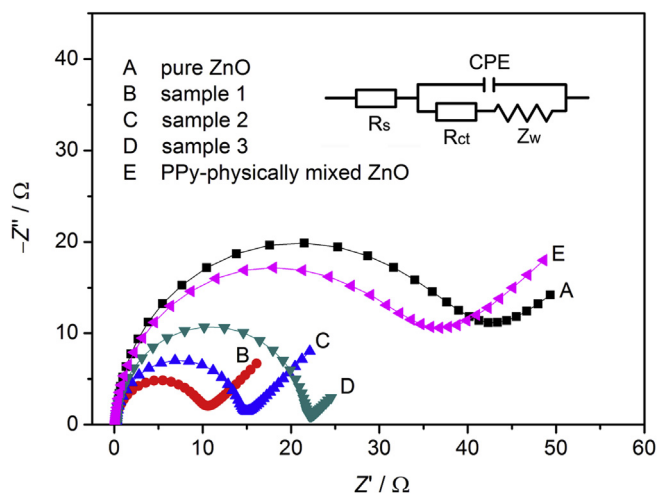

Fig. 10. Electrochemical impedance spectroscopy and Randles equivalent circuit for the zinc electrodes with pure ZnO (curve A), sample 1 (curve B), sample 2 (curve C), sample 3 (curve D) and PPy-physically mixed ZnO (curve E).

initial content of pyrrole, the ZnO crystal structure is almost destroyed by the strong interaction between ZnO and PPy owing to the ultrasonic treatment. SEM and TEM analysis show sample 1 have PPy film around the ZnO cores, but sample 2 and sample 3 possess layer morphology that is different from the morphology of ZnO, in keeping with the result of XRD pattern. Compared to the pure ZnO and PPy-physically mixed ZnO electrode, sample 1 and sample 2 electrodes present superior capacity stability, more stable charge plateau and higher discharge plateau. From CV and EIS analysis, we can know that the stable cycle performance of ZnO/PPy composites is mainly associated to the effective retention of oxidized species on the electrode and the improved mobility of electrons, which can result in small polarization. But for sample 3, the charge/discharge properties deteriorate because of the high diffusive resistance caused by too much content of PPy.

Acknowledgments

References

[1] F.R. McLarnon, E.J. Cairns, J. Electrochem. Soc. 138 (1991) 645–664.
[2] Y.F. Yuan, J.P. Tu, H.M. Wu, B. Zhang, X.H. Huang, X.B. Zhao, Electrochem. Commun. 165 (2006) 653–657.
[3] J. Jindra, J. Power Sources 66 (1997) 15–25.
[4] X.M. Fan, Z.H. Yang, R.J. Wen, B. Yang, W. Long, J. Power Sources 224 (2013) 80–85.
[5] C. Iwakura, H. Murakami, S. Nohara, N. Furukawa, H. Inoue, J. Power Sources 152 (2005) 291–294.
[6] Z.G. Luo, S.B. Sang, Q.M. Wu, S.Y. Liu, ECS Electrochem. Lett. 2 (2013) A21–A24.
[7] L. Zhang, H. Huang, W.K. Zhang, Y.P. Gan, C.T. Wang, Electrochim. Acta 53 (2008) 5386–5390.
[8] Y.F. Yuan, Y. Li, S. Tao, F.C. Ye, J.L. Yang, S.Y. Guo, J.P. Tu, Electrochim. Acta 54 (2009) 6617–6621.
[9] J.Z. Wu, J.P. Tu, Y.F. Yuan, M. Ma, X.L. Wang, L. Zhang, R.L. Li, J. Zhang, J. Alloy. Compd. 479 (2009) 624–628.
[10] S.H. Lee, C.W. Yi, K. Kim, J. Phys. Chem. C 115 (2011) 2572–2577.
[11] D.Q. Zeng, Z.H. Yang, S.W. Wang, X. Ni, D.J. Ai, Q.Q. Zhang, Electrochim. Acta 56 (2011) 4075–4080.
[12] J. Jindra, J. Power Sources 88 (2000) 202–205.
[13] M. Ma, J.P. Tu, Y.F. Yuan, X.L. Wang, K.F. Li, F. Mao, Z.Y. Zeng, J. Power Sources 179 (2008) 395–400.
[14] J.L. Yang, Y.F. Yuan, H.M. Wu, Y. Li, Y.B. Chen, S.Y. Guo, Electrochim. Acta 55 (2010) 7050–7054.
[15] Y.F. Yuan, J.P. Tu, H.M. Wu, Y. Li, D.Q. Shi, Nanotechnology 16 (2005) 803–808.
[16] R.J. Wen, Z.H. Yang, X.M. Fan, Z.Y. Tan, B. Yang, Electrochim. Acta 83 (2012) 376–382.
[17] C.C. Yang, W.C. Chien, P.W. Chen, C.Y. Wu, J. Appl. Electrochem. 39 (2009) 39–44.
[18] X.M. Fan, Z.H. Yang, X.E. Xie, W. Long, R.J. Wang, Z.L. Hou, J. Power Sources 241 (2013) 404–409.
[19] P. Xu, X.J. Han, C. Wang, D.H. Zhou, Z.S. Lv, A.H. Wen, X.H. Wang, B. Zhang, J. Phys. Chem. B 112 (2008) 10443–10448.
[20] Z.H. Guo, K. Shin, A.B. Karki, D.P. Young, R.B. Kaner, H.T. Hahn, J. Nanopart. Res. 11 (2009) 1441–1452.
[21] M. Suga, N. Kuroda, S. Akita, United States Patent 5,348,802, 1995.
[22] J. Vatsalarani, S. Geetha, D.C. Trivedi, P.C. Warrier, J. Power Sources 158 (2006) 1484–1489.
[23] J. Vatsalarani, D.C. Trivedi, K. Ragavendran, P.C. Warrier, J. Electrochem. Soc. 152 (2005) A1974–A1978.
[24] J.L. Zhu, Y.H. Zhou, J. Power Sources 73 (1998) 266–270.
[25] K. Miyazaki, Y.S. Lee, T. Fukutsuka, T. Abe, Electrochemistry 80 (2012) 725–727.
[26] L. Geng, Y. Zhao, X. Huang, S. Wang, S. Zhang, W. Huang, S. Wu, Synth. Met. 156 (2006) 1078–1082.
[27] H.C. Kand, K.E. Geckeler, Polymer 41 (2000) 6931–6934.
[28] S.S. Barkade, D.V. Pinjari, A.K. Singh, P.R. Gogate, J.B. Naik, S.H. Sonawane, M. Ashokkumar, A.B. Pandit, Ind. Eng. Chem. Res. 52 (2013) 7704–7712.
[29] R.W. Powers, M.W. Breiter, J. Electrochem. Soc. 116 (1969) 719–729.
[30] B. Huang, F. Li, Q.C. Yu, G. Chen, B.Y. Zhao, K.A. Hu, J. Power Sources 128 (2004) 135–144.
[31] A. Batool, F. Kanwal, M. Imran, T. Jamil, S.A. Siddiqi, Synth. Met. 161 (2012) 2753–2758.